Journal of New Materials for Electrochemical Systems 13, 163-169 (2010)
© J. New Mat. Electrochem. Systems

Syntghesis and Cheracterization of PdAg Nanoparticles as Oxygen Electrocatalyst in Acidic Medium

Diana C. Martínez-Casillas[1], Gerardo Vazquez-Huerta[1,*], Juan F. Perez-Robles[2], Omar Solorza-Feria[1]

[1] Departamento de Química. Centro de Investigación y de Estudios Avanzados del IPN 2508, C.P.07360, México D.F., México.
[2] Departamento de Materiales. CINVESTAV- IPN. Unidad Querétaro, Querétaro, México.

Received: November 19, 2009, Accepted: January 29, 2010

Abstract: *PdAg electrocatalyst was prepared following two different methods, i.e. borohydride reduction of metallic ions and sonochemistry. X-ray diffraction (XRD) and transmission electron microscopy (TEM) characterizations indicate the formation of crystalline PdAg particles with an average particle size of 10 nm from chemical reduction, and 12 nm from sonochemistry. The electrocatalytic activity of PdAg, for the oxygen reduction reaction (ORR) was characterized using cyclic voltammetry (CV), rotating disk electrode (RDE) and electrochemical impedance spectroscopy (EIS), in 0.5M* H_2SO_4*. Mass-transfered-corrected Tafel plots show an enhancement of the electrocatalytic activity associated to the incorporation of silver to palladium. EIS diagrams of PdAg electrocatalyst present one or two time constants depending on the electrode potential, E. The E at which appears the second time constant depends on the method of catalyst preparation. The difference in E was attributed to the different crystalline percentage due to the catalyst preparation method.*

Keywords: PdAg Electrocatalyst; Oxygen Reduction Reaction; Impedance Spectroscopy.

1. INTRODUCTION

The pollution problems and the future oil scarcity have caused a great amount of investigation in the search of new clean energy sources, without emission of pollutants. The hydrogen-oxygen polymer electrolyte fuel cells, PEMFC, represent a viable option to produce in an efficiently way electric energy, generating only water and heat as by-products. Different metallic electrocatalysts have been extensively studied for PEMFC applications, aiming at the improvement of catalytic activity and stability, at low cost. Also, it is important the development of novel methods of synthesis, which may be easily scaled from laboratory to industry. Among the novel methods is the sonochemistry, which has been used for the synthesis of metallic and bimetallic nanoparticles with good results [1-4].

In a PEMFC, the cathodic oxygen reduction reaction, ORR, is slower than the anodic hydrogen oxidation reaction by several orders of magnitude, thus dominating the overall performance of such fuel cell. Up to now, Pt and its alloys are the most active and stable electrocataysts used for the ORR [5]. However, the high price of platinum and its insufficient availability on the planet limit its use. A lot of work has been focused on the synthesis of novel non-Pt catalysts or at least with lower Pt content, maintaining the activity presented by Pt for the ORR [6]. In this direction, palladium presents an acceptable electrocatalytic activity for the ORR. It has been reported that the ORR proceeds through a 4-electron pathway in acidic medium [7]. Nevertheless, the activity of palladium is smaller than that shown by platinum and ruthenium–based electrocatalysts [6, 10]. The incorporation of different transition metals such as Cu, Co, Ni, Fe to Pd [8 – 13] enhance its performance in comparison with Pd alone [7].

The aim in this work is to study the kinetic and electrochemical properties of the bimetallic alloy, PdAg, as electrocatalyst for the ORR. For this purpose, PdAg electrocatalyst was synthesized using two methodologies *i*) borohydride reduction of $Pd(NO_3)_2{\cdot}2H_2O$ and $AgNO_3$ used as precursors by following a typical methodology [8, 13] and *ii*) using sonochemistry. PdAg catalyst powder was physically characterized using the transmission electron microscopy (TEM) and x-ray diffraction (XRD). Cyclic voltammetry (CV), rotating disk electrode (RDE), and the electrochemical impedance spectroscopy (EIS), were employed in order to evaluate the electrochemical activity and kinetic parameters.

---

*To whom correspondence should be addressed: Email: gervazkez@gmail.com
Phone: +52 (55) 57473800 ext 4473; Fax: +52 (55) 57473389

2. EXPERIMENTAL

2.1. Electrocatalyst Preparation

The PdAg electrocatalyst was produced by two different routes: 1) Chemical reduction of $Pd(NO_3)_2 \cdot 2H_2O$ (0.94 mM) and $AgNO_3$ (0.94 mM) by $NaBH_4$ in a 100 mL tetrahydrofuran (THF) [8, 13]. Briefly, a chemical reactor was loaded with the salts and THF, afterwards the reducing agent ($NaBH_4$, 3.3 mM) was slowly added. A change in color is observed, the change of color is associated to the catalysts formation. 2) Sonochemistry. The reduction of the corresponding Pd and Ag salts assisted with acoustic cavitations cause a sonochemical reaction. Using this technique, the chemical reactor was loaded with $Pd(NO_3)_2 \cdot 2H_2O$ (0.31 mM), $AgNO_3$ (0.31 mM), carbon Vulcan XC-72 and 60 mL of a water/ethylene glycol solution. The system was deareated with N_2 for 10 minutes and then sonicated for 3 hours. During the sonochemical synthesis a nitrogen flux was maintained above the solution. The powders obtained from the chemical reduction and sonochemistry were separately washed and filtered. Subsequently, they were dried at room temperature and maintained in closed vessels prior to physical and electrochemical characterization.

2.2. Physical Characterization

The structural characterization of PdAg was performed using x-ray diffraction (XRD) from a D8 Advance diffractometer (Bruker) equipped with Cu-K_α radiation source (λ =0.15443 nm). XRD patterns were obtained from 30º to 90º of 2θ, with a scan rate of 0.02° min^{-1}. The morphology of PdAg catalyst was observed using transmission electron microscopy (TEM), from a JEOL JEM 1200 EX microscope operating at 120 kV and 70 µA. XRD data were analyzed using the diffractometer´s software, Diffract Plus, and Topas software. XRD patterns were compared with the JCPDS database included in the diffractometer´s software.

2.3. Electrochemical Characterization

The catalytic activity of PdAg was evaluated in a 0.5 mol L^{-1} H_2SO_4 solution, at 25 °C, in a three-electrode electrochemical cell. A platinum mesh was used as counter electrode. Potentials were determined using a Hg/Hg_2SO_4/0.5 M H_2SO_4 (~0.68 V/NHE) reference electrode. A glassy carbon covered with a catalytic ink containing the PdAg catalysts was used as working electrode. PdAg catalytic ink was prepared and deposited on the glassy carbon electrode (geometric area =0.071 cm^2) following a typical methodology reported previously [13- 14]. 4 µl of this ink was deposited onto the glassy carbon disc electrode. The ink was allowed drying at room temperature. The estimated amount of catalyst was about 0.25 mg cm^{-2}. It is worth mentioning that the PdAg electrocatalyst prepared by chemical reduction was supported in carbon Vulcan (20% w/w) during the ink preparation, the same percentage of carbon Vulcan was added during the preparation of PdAg synthesized by sonochemistry.

All the electrochemical studies were performed in a potentiostat/galvanostat (PARSTAT model 2273). Before CV experiments, the sulfuric acid solution was bubbled with N_2 for 30 minutes in order to achieve an oxygen-free aqueous electrolyte. In order to clean and active the electrode surface, 30 oxidation-reduction cycles were performed at 100 mV s^{-1}. The I vs E curves were recorded maintaining the N_2 atmosphere above the electrolyte. Subsequently, the electrolytic solution was saturated with O_2 for 10 min and the hydrodynamic experiments were performed varying the rotation rate of the working electrode within the range of 100 to 900 rpm, at 5 mV s^{-1}. Rotating disc electrode (RDE) tests were performed using a rotor coupled to a rotation-speed controller from Pine Inc. During the ORR measurements, the O_2 flux was maintained constant and above the electrolyte surface.The impedance spectra of PdAg were obtained at different dc potentials (*E*), after prepolarization at the same potential by 180 seconds. During the whole experiment the working electrode was rotating at 1000 rpm. The potential step and the electrode rotation were applied in order to achieve a pseudo steady state. The amplitude of the signal perturbation was 10 mV, the frequency range scanned was from 100 kHz to 10 mHz.

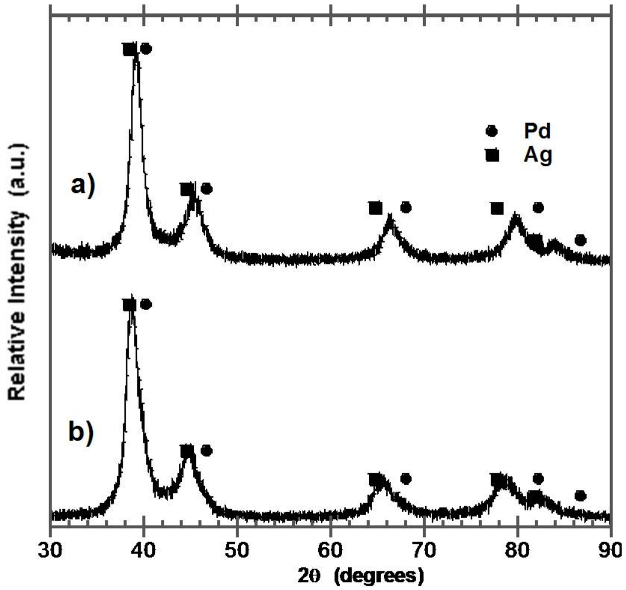

Figure 1. XRD patterns of: a) PdAg synthesized by sonochemistry and b) PdAg synthesized through chemical reduction.

3. RESULTS AND DISCUSSION

3.1. Physical characterization

The x-ray diffraction patterns of PdAg catalyst prepared by two procedures are shown in Figure 1. XRD patterns of PdAg synthesized by chemical reduction and sonochemisty resemble the x-ray diffraction pattern of face-centered-cubic Pd (JCPDS card 046-1043). In both cases (i.e. chemical reduction and sonochemical synthesis), the diffraction peaks of PdAg catalyst are slightly shifted to lower 2θ values with respect to those corresponding to Pd alone due to the formation of the PdAg alloy. The broad feature, at low angles, suggests the presence of nanocrystallites. By using the Topas Academic Software, the crystalline percentage was calculated, giving 41% and 35% for the PdAg prepared by chemical reduction and sonochemistry respectively. On the other hand, the TEM image of PdAg synthesized using sonochemistry shows PdAg particles of about 12 nm (Figure 2a). In Figure 2b, the TEM image of PdAg catalyst synthesized by chemical reduction is shown, the particle size is ~ 10 nm. The insets in Figure 2 correspond to the

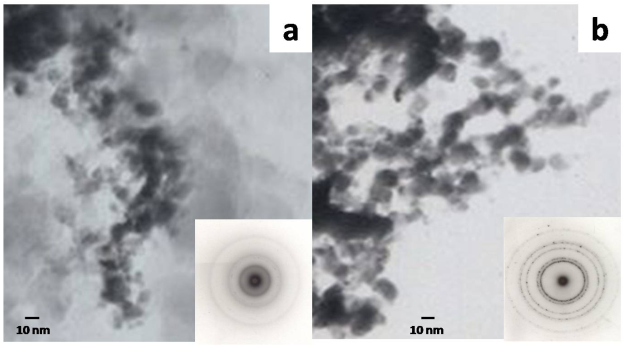

Figure 2. TEM images of synthesized: a) PdAg/C by sonochemistry and b)PdAg by chemical reduction. The insets are the electron diffraction patterns.

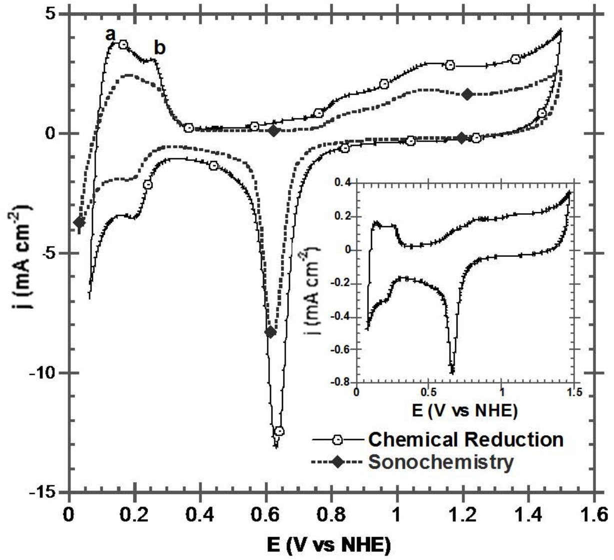

Figure 3. Cyclic voltammograms of PdAg prepared using two different synthesis methods, in N_2-deareated 0.5M H_2SO_4. Scan rate of 100 mV s^{-1}. The inset is the cyclic voltammogram of Pd at the same experimental conditions.

electron diffraction pattern of PdAg prepared by two different procedures. The electron diffraction pattern in the inset of Figure 2a has faded circles, in comparison with the better defined circles of the PdAg prepared by the chemical reduction method (inset of Figure 2b); the better defined circles are associated to the formation of a large number of single crystals — crystallites — and an amorphous phase. The faded circles are caused by the smaller quantity of crystallites and larger amount of the amorphous phase (Figure 2a). This is in agreement with the higher crystalline percentage found from XRD analysis. In order to observe if the higher crystallinity of the PdAg prepared by chemical reduction is reflected on its electrocatalytic activity, different electrochemical tests were performed.

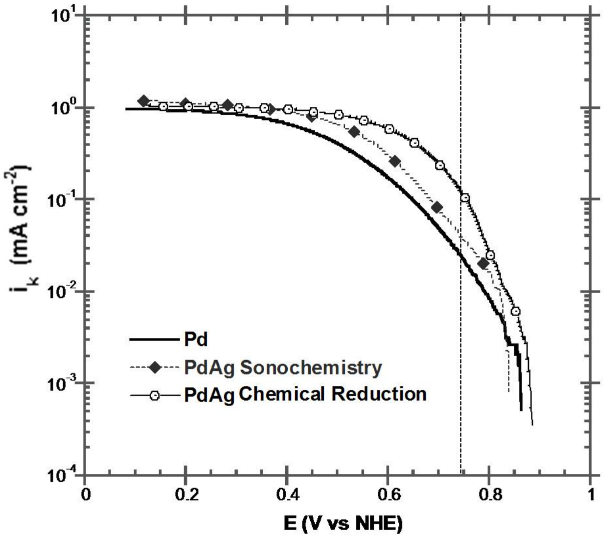

Figure 4. Mass-transfer-corrected Tafel plots of Pd and PdAg prepared with two different methods for the ORR at 25°C.

3.2. Electrochemical characterization

3.2.1. PdAg cyclic voltammograms

Fig. 3 shows the cyclic voltammograms of PdAg prepared following the aforementioned methods. The voltammogram of Pd has been included as inset in the Figure 3 for comparison purposes. As can be observed, the voltammograms are quite similar to that presented for paladium. Also, a higher current value in the double layer region (0.3-0.45 V) and an increase of the oxide reduction current respect to the Pd are observed in PdAg. The hydrogen desorption peaks a and b, in Figure 3, are better defined in the case of PdAg synthesized by chemical reduction method, the definition of peaks a and b must be related to a higher crystallinity of the catalyst. For amorphous catalysts desorption peaks look broader, as in the case of PdAg synthesized by sonochemistry (Figure 3). This result is in agreement with that found in the physical characterization.

3.2.2. RDE measurements

Figure 4 shows the mass-transfer-corrected Tafel plots of PdAg prepared as mentioned before. The kinetic current densities were normalized to the geometrical area of the electrode. Also in Figure 4, the kinetic current density of Pd prepared by chemical reduction is shown only for comparison purposes. The addition of silver to Pd improves its activity towards the ORR. The comparison of current densities between PdAg and Pd alone electrocatalysts at 0.75 V, shows that the highest current density is obtained for PdAg obtained by chemical reduction. Kinetic parameters deduced from Tafel plots are summarized in Table 1. Tafel slope, – b, of about 0.120V dec^{-1} was deduced for both PdAg electrocatalysts, as expected for a first electron transfer as the rate determining step [15, 16]. Values of the exchange current densities, reported in Table 1, are consistent with those reported for nanometric catalysts containing Pd and Ru [13, 14, 17]. The electrocatalytic activity of PdAg towards the ORR is higher in comparison with Pd electrocatalyst, which the enhancement effect can be possibly due to the bifunc-

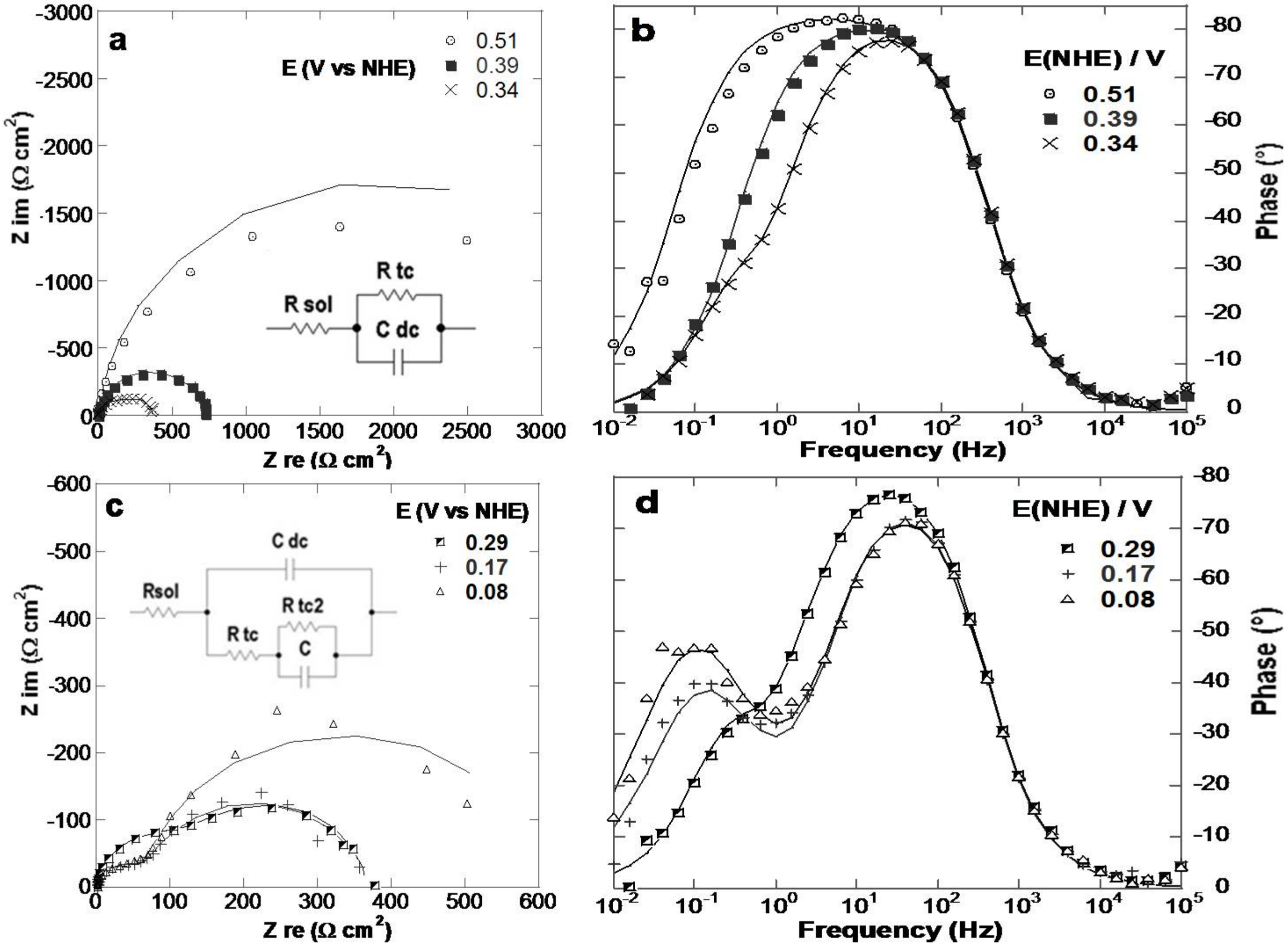

Figure 5. Nyquist and Bode spectra of PdAg synthesized by sonochemistry, the spectra were obtained in an O_2-saturated 0.5M H_2SO_4 electrolyte, different potentials are shown. The insets are the electrical circuits to analyze the impedance response. Rsol is the resistance of the solution (0.98Ω cm^2); Cdc is the double layer capacitance; Rtc is the charge transference resistance of the reduction process from O_2 to H_2O, Rtc2 is the charge transference resistance associated to the reduction of H_2O_2 to H_2O; C is the capacitance of all adsorbed intermediates. The spectra in lines belong to the calculated spectra from the best-fit.

tional effect [18] in which the unique catalytic properties of each of the elements combine in a synergetic form to yield a more active surface than Pd or Ag alone. PdAg electrocatalyst prepared by chemical reduction and sonochemistry were also tested using the electrochemical impedance spectroscopy, in order to obtain more insight in the electrochemical process regarding the mechanism and the kinetics of the ORR.

3.2.3. Impedance characterization of PdAg

The impedance spectra of PdAg were obtained at different dc potentials (E), after pre-polarization at the same electrode potential by 180 seconds. Values of E were within the potential range of 0.80 V and 0.21 V *vs* NHE. The impedance spectra of PdAg synthesized by sonochemistry and chemical reduction methods are shown in Figures 5 and 6, respectively. The impedance diagrams show simi-

Table 1. Kinetic parameters calculated from the mass-transfer-corrected Tafel plots of the ORR on different electrocatalysts in 0.5M H_2SO_4 at 25°C.

	Pd	PdAg Sonochemistry	PdAg Chemical Reduction
-b (V dec^{-1})	0.125	0.126 ± 0.007	0.125 ± 0.004
α	0.47	0.47 ± 0.03	0.47 ± 0.02
$j_0 \times 10^6$ (mA cm^{-2})	3.0	7.1 ± 5.0	13.7 ± 5.0
$i_{k, E=0.75V}$ (mA cm^{-2})	2.1×10^{-2}	3.7×10^{-2}	1.1×10^{-1}

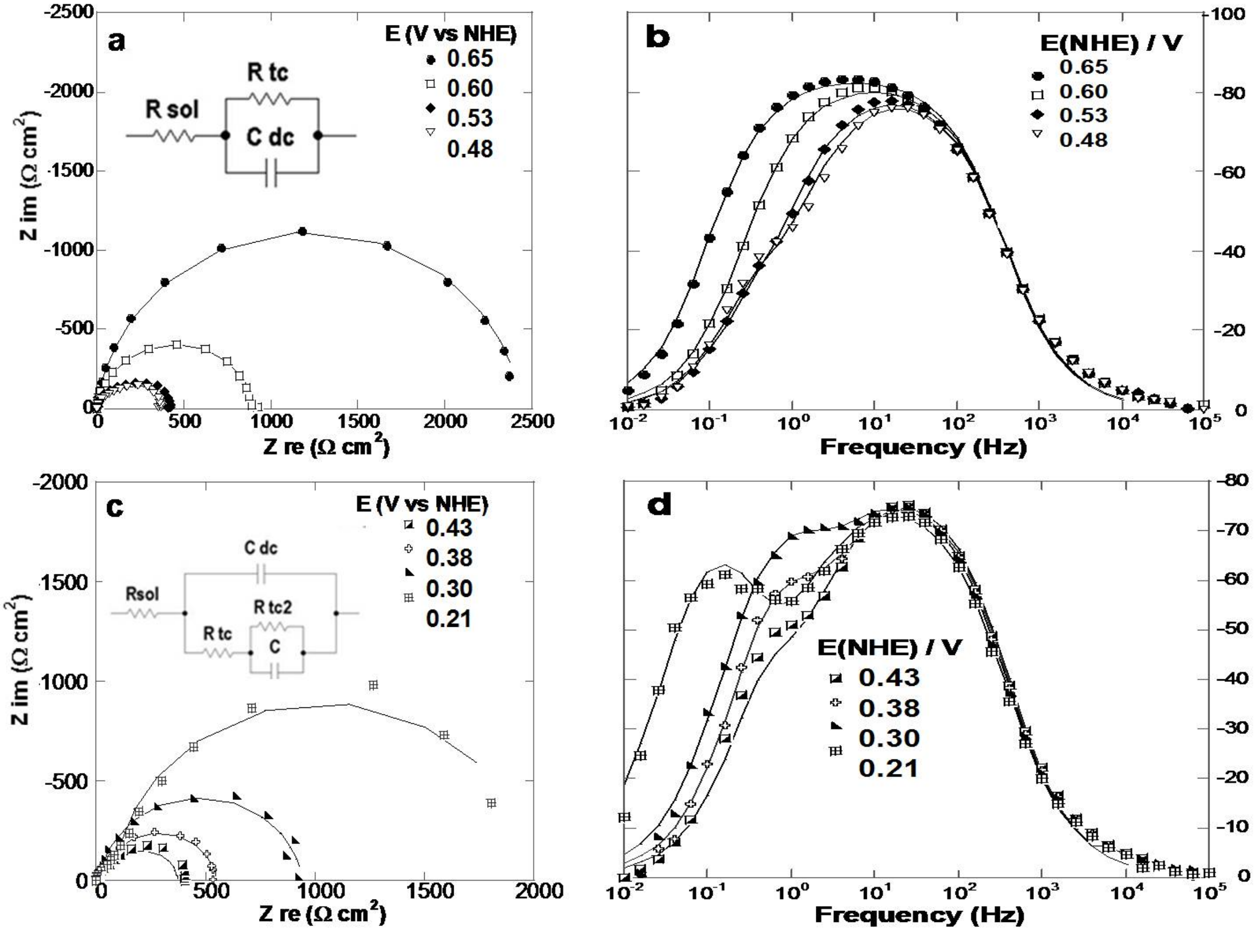

Figure 6. Nyquist and Bode spectra of PdAg synthesized by chemical reduction, the spectra were obtained in an O_2-saturated 0.5M H_2SO_4 electrolyte, different potentials are shown. The insets are the electrical circuits to analyze the impedance response. Rsol is the resistance of the solution (1Ω cm^2); Cdc is the double layer capacitance; Rtc is the charge transference resistance of the reduction process from O_2 to H_2O, Rtc2 is the charge transference resistance associated to the reduction of H_2O_2 to H_2O; C is the capacitance of all adsorbed intermediates. The spectra in lines belong to the calculated spectra from the best-fit.

lar features regardless the method of preparation, two behaviors which depend on E are observed. The impedance spectra of PdAg prepared by sonochemistry, and for E > 0.34V, present one loop associated to the time constant of a single process. (Figure 5a and 5b, respectively), the real and imaginary components of impedance decrease as the potential becomes more negative. Nevertheless, the curves always show a single time constant within this potential range. In contrast, for E ≤ 0.34 V *vs* NHE, the Nyquist and Bode diagrams show two loops (Figures 5c and 5d) associated to two time constants. The first time constant is observed in the middle frequency range, while the second at low frequencies. The first time constant can be associated to the reduction process from O_2 to H_2O via 4e-, this reaction is usually reported for palladium [7] and Pd-based electrocatalysts [8, 13]. However, by using scanning electrochemical microscopy (SECM) C. M. Sánchez and A. J. Bard have found that H_2O_2 is produced at different materials (i.e. Hg, Au, Ag, Cu, Pd, and $Au_{60}Cu_{40}$) tested as electrocatalysts for the oxygen reduction reaction (ORR), in 0.5 M H_2SO_4. The materials show intermediate values (between 2-4) of transferred electrons as a function of potential [19]. The quantity of H_2O_2 can be related to the total number of electrons, n, with n = 2 only H_2O_2 is generated, while n = 4 indicates H_2O formation. The intermediate values of n, between 2 to 4 may be associated to the formation of intermediate species such as OH_{ads} and O_2H_{ads}. [20]. The second time constant, detected during the impedance measurements in Figure 1c and d, may be caused by the reduction of H_2O_2 to H_2O by assuming that H_2O_2 is the majoritarian intermediate specie [19,21], even though the other adsorbed intermediate species may have some interference on the low frequency loop.

The Nyquist and Bode spectra of PdAg synthesized by chemical reduction (Figure 6) present a quite similar behavior with potential like that shown by PdAg produced using sonochemistry. However, the E at which the second time constant appears differs in approximately 0.14 V being the catalyst synthesized by chemical reduction more positive. This fact indicates the different nature of PdAg electrocatalysts prepared by the two different methods. Since the kinetic of adsorption/reduction of H_2O_2 depends on the size and crystal structure of the electrocatalyst particle, the kinetic of the ORR

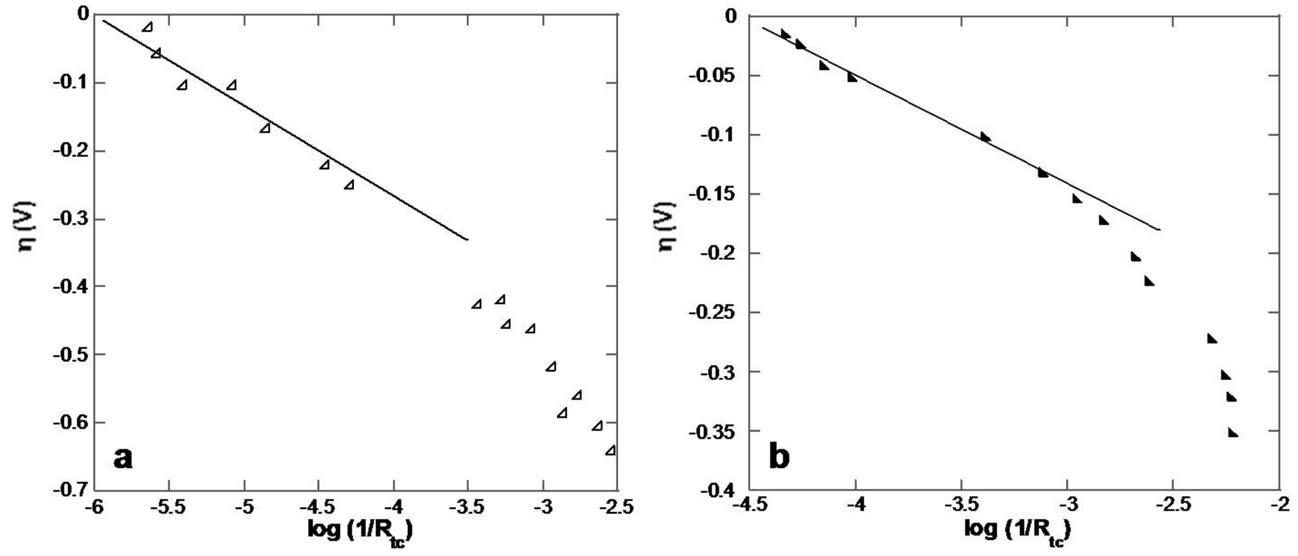

Figure 7. Variation of η vs Log 1/Rtc in a 0.5M H_2SO_4 solution previously saturated with O_2: a)PdAg synthesized by sonochemistry and b) PdAg synthesized by chemical reduction.

must be related with these small differences. That means that even though both methods of preparation produce similar crystalline PdAg electrocatalyst, the higher crystallinity of PdAg prepared by chemical reduction slightly enhances its electrochemical activity for the ORR.

In order to obtain quantitative information concerning the processes involved in the mechanism of the ORR on PdAg catalyst, two electric circuits (insets from Figures 5 and 6) were employed for fitting the impedance diagrams. By using the Boukamp EQIVCT fitting program [22], the values for all the elements in the circuits were obtained. However, only the values of Rtc are presented. The values of Rtc represent the values of the charge transfer resistance for the reduction process from O_2 to H_2O. The Rtc values obtained from the fit can be used to determine the ORR kinetic parameters and these values may be compared with those obtained in RDE measurements. Figure 7 shows the behavior $\eta = E - E_{ocp}$ versus Log $1/R_{tc}$, (E_{ocp} is the open circuit potential ~ 0.8 V *vs* NHE). Kinetic parameters deduced from Figure 7 plots are summarized in Table 2. The values of b and a are in good agreement with those obtained in this work from EDR measurements.

4. CONCLUSIONS

PdAg electrocatalyst was prepared following two different syntheses, *i.e.* by a borohydride chemical reduction and sonochemistry assisted method. The physical characterization indicates the formation of PdAg nanoparticles with an average size particle of 12 and 10 nm for PdAg prepared by sonochemistry and chemical reduction, respectively. The electrochemical studies show that both materials have electrocatalytic activity toward the ORR. The hydrogen adsorption/desorption peaks, in Figure 3, are better defined in the case of PdAg synthesized by chemical reduction method, the higher definition of the adsorption/desorption peaks was associated to a higher crystallinity. On the other hand, the EIS diagrams for the electrocatalysts present one or two time constants depending on the applied E. The first time constant of impedance spectra was associated to the reduction process from O_2 to H_2O, while the second one to the reduction of H_2O_2 to H_2O. The second time constant appears at different E depending on the preparation method of the PdAg electrocatalyst. The difference in E was attributed to the different crystallinity of the PdAg prepared by the two different methods.

Table 2. Kinetic parameters deduced from impedance diagrams from the ORR on PdAg in H_2SO_4 at 25°C.

	PdAg Sonochemistry	PdAg Chemical Reduction
-b ($V\ dec^{-1}$)	0.128	0.126
α	0.46	0.47

5. ACKNOWLEDGEMENTS

This research project was partially supported by a Grant of National Science and Technology Council of Mexico, CONACYT (Ref. 83247) and by the Mexico City Science and Technology Institute, ICYTDF (OSF). DCMC thanks to CONACYT for doctoral fellowship. GVH thanks the financial support from CONACYT through a postdoctoral grant. The authors acknowledge to Juan Antonio Jimenez, Carlos Flores and Dr. José Chavez for the technical assistance in XRD and TEM measurements.

REFERENCES

[1] K. Okitsu, Y. Mizukoshi and H. Bandow, Ultrason. Sonochem., 3, S249 (1996).
[2] R. A. Salkar, P. Jeevanandam and S.T. Aruna, Langmuir, 15, 2733 (1996).
[3] T. Fujimoto, S. Terauchi and H. Umehara, Chem. Mater., 13, 1057 (2001).
[4] R. Oshima, T.A. Yamamoto and Y. Mizukoshi, Nanostruct.

Mater., 12, 111(1999).

[5] M. Gustavsson, H. Ekstroem, P. Hanarp, G. Lindbergh, E. Olsson and B. Kasemo, J. Power Sources, 163, 671 (2007).

[6] H.A. Gasteiger, S.S. Kocha, B. Sompalli, F.T. Wagner, Applied Catalysis: environmental 56, 9 (2005).

[7] J.J. Salvador-Pascual, S. Citalán-Cigarroa, O. Solorza-Feria, J. Power Sources, 172, 229 (2007).

[8] C. Xu, Y. Zhang, L. Wang, L, Xu, X, Bian, H. Ma and Y. Ding, Chem. Mater., 21, 3110 (2009).

[9] J.L. Fernández, D.A. Walsh, A.J. Bard, J. Am. Chem. Soc., 127, 357 (2005).

[10]K. Suárez-Alcántara, O. Solorza-Feria, Fuel Cells, in press 2009.

[11]K. Lee, O. Savadogo, A. Ishihara, S. Mitsushima, N. Kamiya and K.-I. Ota, J. Electrochem. Soc., 153, A20 (2006).

[12]M. Shao, P. Liu, J. Zhang and R. Adzic, J. Phys. Chem.B, 111, 6772 (2007).

[13]G. Ramos-Sánchez, H. Yee-Madeira, O. Solorza-Feria, Int. J. Hydrogen Energy, 33, 3596 (2008).

[14]R.G. González-Huerta, A. Chávez-Carvayar and O. Solorza-Feria, J. Power Sources, 153, 11 (2006).

[15]Allen J. Bard and Larry R. Faulkner, Electrochemical Methods: Fundamentals and Applications, 2nd edition, John Wiley & Sons, Inc., USA, 2001.

[16]E. Yeager, Electrochimica Acta, 92, 1527 (1984).

[17]K. Suárez-Alcántara, O. Solorza-Feria, J. Power Sources, 192, 165 (2009).

[18]H. Liu, A. Manthiram, Energy and Environmental Science, 2, 124 (2009).

[19]C.M. Sanchez-Sánchez, A.J. Bard. Anal. Chem., 81, 8094 (2009).

[20]K. Kinoshita, Electrochemical Oxygen Technology, Wiley-Interscience Publication, New York, (1992).

[21]L. Zhang, K. Lee, J. Zhang, Electrochim Acta, 52, 3088 (2007).

[22]Bernard A. Boukamp. Solid State Ionics, 20, 31 (1986).